

See discussions, stats, and author profiles for this publication at: <https://www.researchgate.net/publication/231402811>

Fullerene formation in sputtering and electron beam evaporation processes

ARTICLE *in* THE JOURNAL OF PHYSICAL CHEMISTRY · APRIL 1992

DOI: 10.1021/j100196a005

CITATIONS

43

READS

17

9 AUTHORS, INCLUDING:



Shyankay Jou

National Taiwan University of Science and Te...

32 PUBLICATIONS 334 CITATIONS

SEE PROFILE



Lyle Isaacs

University of Maryland, College Park

159 PUBLICATIONS 7,659 CITATIONS

SEE PROFILE



Chahan Yeretzian

Zurich University of Applied Sciences

89 PUBLICATIONS 2,000 CITATIONS

SEE PROFILE

Conclusions

A TICT state with fast radiationless deactivation is formed by rotamerism around the central single bond in [(dimethylamino)phenyl]methylpyridinium. Suppression of rotamerism enhances the yield of fluorescence by orders of magnitude.

Similar nonfluorescent TICT states are formed in homologs with a double bond between aniline and pyridine or with derivatives of naphthalene as donor and acceptor.^{5,21} These dyes are used as voltage-sensitive fluorescence probes in neuron membranes.² By suppression of rotamerism we may expect to obtain voltage-sensitive probes with a high yield of fluorescence, i.e., an enhanced signal-to-noise ratio at given conditions of staining and illumination.

Acknowledgment. We thank Dr. C. Röcker for measuring fluorescence lifetimes and Uwe Theilen for technical assistance. The project was supported by the Deutsche Forschungsgemeinschaft (Grant Fr 349/5) and by the Fonds der Chemischen Industrie.

References and Notes

- (1) Cohen, L. B.; Leshner, S. In *Optical Methods in Cell Physiology*; de Weer, P., Salzberg, B. M., Eds.; Wiley: New York, 1986; p 71.
- (2) Fromherz, P.; Dambacher, K. H.; Ephardt, H.; Lambacher, A.; Müller, C. O.; Neigl, R.; Schaden, H.; Schenk, O.; Vetter, T. *Ber. Bunsen-Ges. Phys. Chem.* **1991**, 95, 1333.
- (3) Fromherz, P.; Vetter, T. *Proc. Natl. Acad. Sci. U.S.A.* **1992**, 89, 2041.
- (4) Fromherz, P.; Lambacher, A. *Biochim. Biophys. Acta* **1991**, 1068, 149.
- (5) Ephardt, H.; Fromherz, P. *J. Phys. Chem.* **1989**, 93, 7717.
- (6) Ephardt, H.; Fromherz, P. *J. Phys. Chem.* **1991**, 95, 6792.
- (7) Grabowski, Z. R.; Rotkiewicz, K.; Siemiarz, A.; Cowley, J.; Baumann, W. *Nouv. J. Chim.* **1979**, 3, 343.
- (8) Fuson, R. C.; Miller, J. A. *J. Am. Chem. Soc.* **1957**, 79, 3477.
- (9) Péron-Roussel, O.; Jacquignon, M. P. C. R. Acad. Sci. Paris C **1974**, 278, 279.
- (10) Reichardt, C.; Kaufmann, N. *Chem. Ber.* **1985**, 118, 3424.
- (11) Migachev, G. I.; Stepanov, B. I. *J. Gen. Chem. USSR* **1968**, 38, 1320.
- (12) Bergmann, E. D.; Crane, F. E.; Fuoss, R. M. *J. Am. Chem. Soc.* **1952**, 74, 5979.
- (13) Olmsted III, J. J. *J. Phys. Chem.* **1979**, 83, 2581.
- (14) The fluorescence yield in chloroform ($\Phi_F = 1.5\%$ at $\epsilon = 4.72$) is by a factor of 10 lower than expected from the general trend in Figure 1. The solubility of the dye in chloroform is low. Selective solvation by ethanol—present in all solutions at a volume fraction of 0.3%—may play a significant role.
- (15) Strickler, S. J.; Berg, R. A. *J. Chem. Phys.* **1962**, 37, 814.
- (16) Lifetime and quantum yield of fluorescence for dye I in methanol are $\tau_F = 2.0$ ns and $\Phi_F = 0.28$. We obtain $k_F = \Phi_F/\tau_F = 0.14$ ns⁻¹. For an analog of dye II [(dibutylamino)phenyl]pyridinium butylsulfonate in methanol, we obtained from $\tau_F = 150$ ps and $\Phi_F = 0.01$ a value $k_F = \Phi_F/\tau_F = 0.16$ ns⁻¹.⁶
- (17) The spectra of dye II are identical to those of [(dimethylamino)phenyl]pyridinium butylsulfonate and very similar to those of [(dibutylamino)phenyl]pyridinium butylsulfonate.⁶ The solvatochromism is independent on the counterion. It is a sole property of the charged chromophore itself.
- (18) Dewar, M. J. S.; Thiel, W. J. *J. Am. Chem. Soc.* **1977**, 99, 4899.
- (19) Stewart, J. J. P. *MOPAC Manual*, 2nd ed.; University of Texas: Austin, TX; QCPE No. 455.
- (20) Rettig, W.; Majenz, W.; Lapouyade, R.; Haucke, G. *J. Photochem. Photobiol. A: Chem.* **1992**, 62, 415.
- (21) Ephardt, H.; Fromherz, P., manuscript in preparation.

Fullerene Formation in Sputtering and Electron Beam Evaporation Processes

Rointan F. Bunshah,* Shyankay Jou, Shiva Prakash, Hans J. Doerr,

Department of Material Sciences and Engineering, University of California, Los Angeles, California 90024-1595

Lyle Isaacs, Arno Wehrsig, Chahan Yeretzian, Hyunhae Cynn,

Department of Chemistry and Biochemistry, University of California, Los Angeles, California 90024-1569

and François Diederich*

Laboratorium für Organische Chemie, ETH-Zentrum, Universitätsstrasse 16, CH-8092 Zürich, Switzerland
(Received: May 24, 1992; In Final Form: June 30, 1992)

We report the formation of fullerenes from graphite by sputtering and electron beam evaporation. Under conditions that differ dramatically from those in the previously known fullerene production processes, the new methods preferentially yield the soluble higher fullerenes C₇₀, C₇₆, C₇₈, and C₈₄ in addition to minor amounts of C₆₀ only. Upon passage of carbon particles formed by electron beam evaporation through an electrostatic field, fullerenes are mainly isolated from the cathode, not from the anode, which supports the formation of cationic intermediates in fullerene growth mechanisms. The variables thought to be important for fullerene production can be controlled efficiently in the new processes.

Introduction

The availability of gram quantities of C₆₀ by resistive^{1,2} or arc heating³ of graphite has led to a period of intense ongoing research into the chemical, physical, and materials properties of this first molecular allotrope of carbon.^{4,5} In addition to C₆₀ (≈60–70%), the toluene-extractable fraction of the carbon soot formed in both the resistive and arc heating processes contains C₇₀ (20–30%) and approximately 5% of higher fullerenes in the range between C₇₆ and C₉₆.⁶ The isolation of the higher fullerenes, e.g., D₂-C₇₆, C_{2v}-C₇₈, and D₃-C₇₈, from this mixture is tedious and yields only limited amounts of pure material, which explains why the properties of these carbon spheres remain almost entirely unexplored. Since first investigations now show that the chemistry of the higher fullerenes promises to be diverse and distinctively different from the chemistry of buckminsterfullerene and C₇₀,⁷ a search for new fullerene preparations yielding preferentially the higher derivatives

represents a worthwhile research target. Besides the commonly used resistive and arc heating processes, fullerene preparations by laser vaporization of a rotating graphite target in a tube furnace⁸ and by inductive heating of graphite powder⁹ have been reported. In both processes, C₆₀ is by far the predominant product. Different C₆₀/C₇₀ ratios have been isolated from the soot produced in oxidizing benzene flames and, depending on the conditions, variation of the C₇₀/C₆₀ ratio over the range 0.26–5.7 was achieved.¹⁰ We now report that fullerenes are formed by vaporization of graphite in sputtering and electron beam evaporation processes and that both methods consistently yield preferentially C₇₀ and the higher fullerenes with only minor amounts of C₆₀.

Experimental Section

The experimental setup for fullerene growth in sputtering processes is shown in Figure 1. A 7.6-cm-diameter graphite target

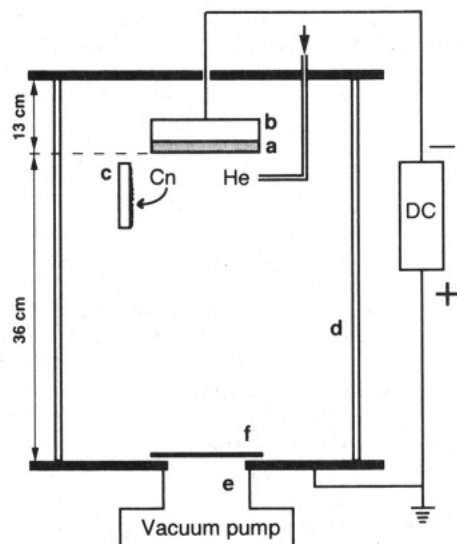


Figure 1. Schematic diagram of the sputtering system used for fullerene generation: 7.6-cm-diameter graphite target (a) attached to a magnetron sputtering cathode (b); liquid nitrogen cooled 12×16.5 cm copper plate (c); 30-cm-diameter Pyrex chamber (d), aperture to vacuum pump (e) partially covered by stainless steel plate (f).

is attached to a magnetron sputtering cathode, whose magnetic field confines the electrons in the vicinity of the target. At a target circuit power of 2.5 kW, carbon species are sputtered from the graphite target by helium ions from the discharge between the cathode target assembly and a ground plate located 36 cm away at the bottom of the vacuum chamber. A lateral flow of helium close to the graphite target surface serves to cool the sputtered carbon species and to push the material formed toward a liquid nitrogen cooled copper plate placed in the path of the gas flow. The gas flow is adjusted to maintain a helium pressure of 3 Torr in the glass bell jar. Some carbon soot is also collected on the bell jar, which is maintained at room temperature. To prevent the loss of gaseous fullerenes or other carbon species, the opening to the vacuum pump is partially covered by a stainless steel plate. During the sputtering process, a strong glow from the anode plate to the graphite target is visible. However, no high-current arcing occurs as no reduction in the power supplied to the target is observed.

In the electron beam evaporation experiment (Figure 2), a 10-kV electron beam from a 270° deflection electron gun was used to evaporate carbon from a 2.5-cm-diameter POCO graphite rod. The electron beam emission current was 0.2 A, which is necessary to maintain a high evaporation rate, a condition critical for fullerene formation. The base pressure in the stainless steel bell jar was 4×10^{-6} Torr. The operating pressure was 2×10^{-5} Torr without the introduction of any working gas. The flux of carbon species characterized by a high mean free path was made to pass through an aperture in a horizontal plate. Behind the aperture, substrates (quartz, silicon, or copper) to collect charged carbon species are clamped to two electrodes 5.5 cm apart. The substrates are heated from the backside with Quartz lamps to 200 °C. A 1000-V potential was applied between the anode and cathode which deviates charged particles in the direct beam for collection on the electrode substrates. Above the aperture, a liquid nitrogen cooled copper plate was placed to collect the carbon soot from the portion of the direct beam which was not deviated by the electrostatic field. Species in this beam are either neutral or charged but of too high energy to be deviated efficiently in the electrostatic field. In each experiment, the evaporation led to the formation of a conic hole in the graphite rod of approximately 5 mm depth and 10 mm opening diameter at the surface.

The carbon soot collected from the sputtering and electron beam evaporation experiments was extracted with hot toluene and filtered through a plug of cotton to remove particulate matter. The samples were concentrated by rotary evaporation. The HPLC analysis on a Vydac C₁₈ reversed-phase column using toluene:

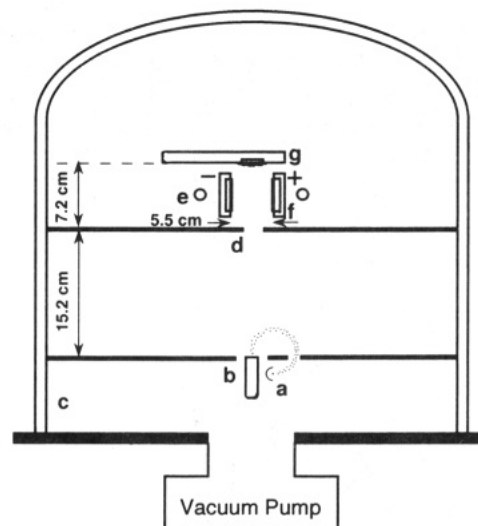


Figure 2. Schematic diagram of the electron beam evaporation system for fullerene production: (a) 270° deflection electron gun; (b) 2.5-cm-diameter POCO graphite rod; (c) 61-cm-diameter water-cooled stainless steel chamber; (d) 2.5×7.6 cm aperture; (e) quartz lamps for radiative heating of substrates on electrodes; (f) electrodes with clamped-on quartz, silicon, or copper substrates; (g) liquid nitrogen cooled copper plate.

acetonitrile (1:1, v/v)⁶ as the eluent showed the predominance of C₇₀ in all samples produced by sputtering and in the samples collected in the electron beam evaporation system from the top copper plate and the quartz substrate on the cathode. In addition to C₇₀, a significant amount of higher fullerenes and only a minor quantity of C₆₀ are isolated in each case. In most runs, the quantity of the soluble higher fullerenes in the range between C₇₆ and C₈₄ equals or exceeds the amount of C₆₀ formed. Figure 3A shows the HPLC trace of material collected from the copper substrate in the sputtering system. Figure 3B shows the HPLC trace of material collected from the cathode in the electron beam evaporation system. In contrast to the results on the cathodic side, only traces of fullerenes are detected on the quartz substrate clamped to the anode. The identity of the fullerenes was confirmed by HPLC comparisons with pure standards and by laser desorption time-of-flight (LD-TOF) mass spectrometry. In both production processes, each run yielded micromolar fullerene quantities, and the total amount of isolated fullerenes was in the milligram range. The approximate yield of fullerenes in the range between C₇₀ and C₈₄ is 0.5% of the total collected material. This should substantially increase with optimization of the deposition variables. In addition to the soluble fullerenes, large amounts of insoluble fullerene soot are isolated, and this material still awaits analysis.

Results and Discussion

Electron beam evaporation deposition and sputter deposition are the basic physical vapor deposition (PVD) processes used extensively for thin film deposition.^{11,12} In the former, thermal energy is used to transform the condensed phase into the vapor. In the latter, positive ion bombardment of the negatively biased sputtering target results in ejection of the target atoms into the gas via momentum transfer. Typical pressure ranges of operation for thin-film deposition for the two processes are 10^{-3} – 10^{-10} Torr (evaporation deposition), $(20\text{--}120) \times 10^{-3}$ Torr of inert gas (diode sputtering), and $(1\text{--}5) \times 10^{-3}$ Torr of inert gas (magnetron sputtering).

These processes can also be used for the deposition of ultrafine particles (UFPs) in the size range from 10 to 100 nm.^{13,14} To this end, the evaporated or sputtered atoms must undergo numerous gas-phase collisions to form clusters, i.e., the mean free path is very small and of the order of 0.1 mm. This is accomplished by maintaining a high pressure of the inert gas in the chamber. Typical pressures for gas-phase condensation are 0.2 to several Torr.

The electron beam evaporation and sputtering processes were now explored for the synthesis of fullerenes, and the experimental

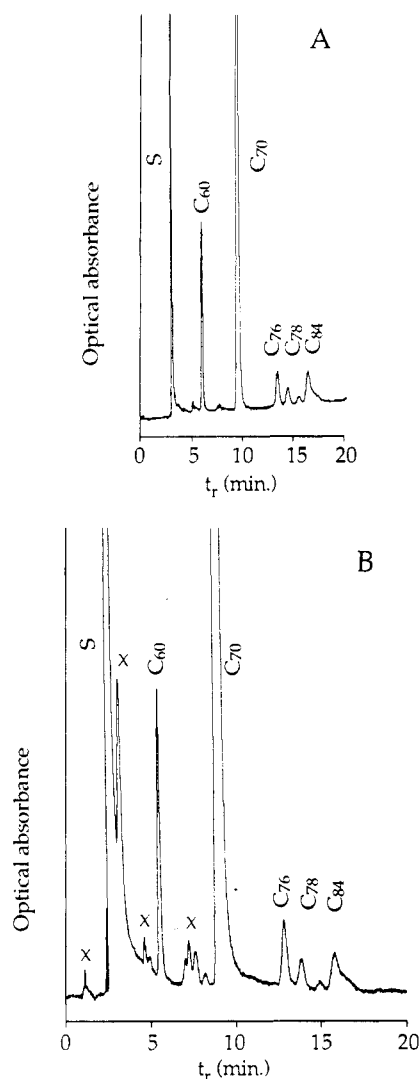


Figure 3. HPLC profiles (C_{18} reversed phase, acetonitrile/toluene (1:1, v/v), 310-nm UV detection) of the toluene-soluble extract of the fullerene soot collected (A) from the copper plate in the sputtering system and (B) from the quartz substrate on the cathode in the electron beam evaporation system. X = unknown impurities; S = solvent.

setups for both methods are shown in Figures 1 and 2. The produced fullerene soot was collected and the toluene-soluble extract worked up and analyzed by HPLC (Figure 3) and LD-TOF mass spectrometry as previously described.⁶ The following results were obtained:

(1) Isolable amounts of fullerenes are formed both in the electron beam evaporation and the sputtering experiments. This is particularly remarkable in view of the pressure conditions in both systems. Whereas the known macroscopic production processes starting from graphite require a helium atmosphere of ≈ 100 –200 Torr for high yields of fullerenes, the sputtering system is maintained under a He pressure of 3 Torr and the bell jar in the electron beam evaporation is kept under high vacuum (2×10^{-5} Torr). Forming macroscopic quantities of fullerenes under these dramatically different conditions suggests that the range of methods producing these carbon spheres from graphite or amorphous carbon substrates may actually be much larger than previously anticipated.

(2) Buckminsterfullerene, C_{60} , clearly is not the prominent species in the two new production processes as shown by the HPLC profiles of typical runs. Figure 3A shows the fullerene mixture isolated from the carbon soot collected from the copper substrate in the sputtering system. By far the most abundant fullerene in the mixture is C_{70} (70% relative integrated intensity), followed by C_{60} (12%), C_{84} (9%), C_{76} (5%), C_{2v} - C_{78} (3%), and D_3 - C_{78} (1%). In some samples, ratios of C_{70}/C_{60} as high as 95:5 have been observed. The distribution of the higher fullerenes between C_{76}

and C_{84} closely resembles the fullerene distribution in the soot produced at UCLA by resistive heating of graphite.⁶

Figure 3B shows the HPLC profile of the fullerenes isolated from the cathodic quartz substrate in the electron beam evaporation process. Again, C_{70} is by far the dominant product (77% relative integrated intensity), followed by C_{60} (9%), C_{84} (6%), C_{76} (5%), C_{2v} - C_{78} (2%), and D_3 - C_{78} (1%). A similar product distribution is isolated from the copper plate which collects the products that are not deviated by the electrostatic field. In contrast to the results on the cathodic site, no significant amounts of fullerenes were found on the anodic substrate.

(3) The observation that fullerenes are isolated from the cathode but not to a significant extent from the anode in the electron beam evaporation system suggests the intermediacy of cationic species in the fullerene growth mechanism. These data add to previous experimental support for cationic pathways to the carbon spheres. In laser desorption Fourier transform mass spectrometric studies, gas-phase ion-molecule reactions lead from the acetylenic all-carbon molecules cyclo[18]carbon (C_{18}) and cyclo[24]carbon (C_{24}) to the fullerene ion C_{70} and from cyclo[30]carbon (C_{30}) to C_{60} .¹⁵ These processes can be observed only in the positive-ion mode and not in the negative-ion mode. Similarly, recent LD-TOF coalescence experiments show that the intensity of the C_{118} ion, formed by coalescence of two C_{60} ions followed by C_2 loss, is many orders of magnitude stronger in the positive than in the negative-ion mode.¹⁶ The relevance of cationic intermediates in fullerene growth processes has its parallel in the chemistry of cage hydrocarbons, where cationic rearrangements on the $C_{10}H_{10}$ hypersurface lead to adamantane and on the $C_{20}H_{20}$ surface to dodecahedrane.¹⁷

(4) Already, the new methods are competitive to the resistive and arc heating production processes for the isolation of C_{70} and, in particular, the higher fullerenes between C_{76} and C_{84} : no tedious chromatographic removal of large quantities of C_{60} is needed. The efficient control over the experimental parameters in these systems should allow us to further enhance the yields of specific fullerenes and to gain novel insights into the mechanism of fullerene growth. The electron beam evaporation process offers the capability of collecting charged carbon species deviated in electrostatic fields of various magnitudes and at varying distance from the graphite source. The sputtering process allows controlled variations of the power in the target circuit, the pressure during operation, the gas flow rate, the temperature of the cooling gas, the temperature of the substrate, and the location of particle collection, i.e., the residence time of the particles in the gas phase.

Conclusion

The application of electron beam evaporation and sputtering of graphite to the production of fullerenes has generated a series of surprising new findings.¹⁸ Both methods lead to macroscopic isolable quantities of fullerenes at pressure conditions that differ dramatically from those applied in the other fullerene production methods which start from graphite. Sputtering produces fullerenes at a He pressure of 3 Torr with electron beam evaporation at high vacuum (2×10^{-5} Torr), conditions that contrast sharply with the 100–200 Torr of He pressure applied in the common resistive and arc heating processes. Buckminsterfullerene is not a special compound under the new production conditions; rather, the formation of C_{70} is strongly preferred. In addition, the higher soluble fullerenes in the range between C_{76} and C_{84} are formed in equal or even larger amounts than C_{60} . The isolation of fullerenes from a cathodic substrate and not from the anodic counterpart in the electron beam evaporation process provides new experimental support for the intermediacy of cationic intermediates in fullerene growth processes. The efficient control of the experimental parameters in the new techniques should make them important probes into the mechanisms of fullerene production and allow a further optimization of their preparative utility.

Acknowledgment. This work was supported by the Office of Naval Research. We thank the U.S. Department of Defense (DOD) for a predoctoral fellowship to L.I., the Fond der Chemischen Industrie, FRG, for a postdoctoral fellowship to A.W., and

the Schweizer Nationalfond for a postdoctoral fellowship to C.Y. We thank Professor Robert L. Whetten for helpful discussions.

References and Notes

- (1) Krätschmer, W.; Lamb, L. D.; Fostiropoulos, K.; Huffman, D. R. *Nature* **1990**, *347*, 354.
- (2) Ajie, H.; Alvarez, M. M.; Anz, S. J.; Beck, R. D.; Diederich, F.; Fostiropoulos, K.; Huffman, D. R.; Krätschmer, W.; Rubin, Y.; Schriver, K. E.; Sensharma, D.; Whetten, R. L. *J. Phys. Chem.* **1990**, *94*, 8630.
- (3) Haufler, R. E.; Conceicao, J.; Chibante, L. P. F.; Chai, Y.; Byrne, N. E.; Flanagan, S.; Haley, M. M.; O'Brien, S. C.; Pan, C.; Xiao, Z.; Billups, W. E.; Ciufolini, M. A.; Hauge, R. H.; Margrave, J. L.; Wilson, L. J.; Curl, R. F.; Smalley, R. E. *J. Phys. Chem.* **1990**, *94*, 8634.
- (4) Kroto, H. W.; Allaf, A. W.; Balm, S. P. *Chem. Rev.* **1991**, *91*, 1213.
- (5) The March 1992 issue of *Acc. Chem. Res.* (**1992**, *25*, 97–175) is entirely dedicated to fullerene research and describes the chemistry and physics of these new carbon allotropes in 11 review articles written by various authors.
- (6) Diederich, F.; Whetten, R. L. In ref 5, pp 119–126.
- (7) Li, Q.; Wudl, F.; Thilgen, C.; Whetten, R. L.; Diederich, F. *J. Am. Chem. Soc.* **1992**, *114*, 3994.
- (8) Smalley, R. E. In ref 5, pp 98–105.
- (9) Peters, G.; Jansen, M. *Angew. Chem.* **1992**, *104*, 240; *Angew. Chem., Int. Ed. Engl.* **1992**, *31*, 223.
- (10) Howard, J. B.; McKinnon, J. T.; Makarovskiy, Y.; Lafleur, A. L.; Johnson, M. E. *Nature* **1991**, *352*, 139.
- (11) Maissel, L. I.; Glang, R., Eds. *Handbook of Thin Film Technology*; MacGraw-Hill: New York, 1970.
- (12) Bunshah, R. F., Ed. *Deposition Technologies for Films and Coatings*; Noyes Publications: Park Ridge, NJ, 1982.
- (13) Hayashi, C. *Phys. Today* **1987**, *40*, 44.
- (14) Suh, T. G.; Umarjee, D. M.; Prakash, S.; Doerr, H. J.; Deshpandey, C. V.; Bunshah, R. F. *Surf. Coatings Technol.* **1991**, *49*, 304–310.
- (15) (a) Rubin, Y.; Kahr, M.; Knobler, C. B.; Diederich, F.; Wilkins, C. L. *J. Am. Chem. Soc.* **1991**, *113*, 495. (b) Ross, M. M.; McElvany, S.; Goroff, N.; Rubin, Y.; Diederich, F., manuscript in preparation.
- (16) Yeretizian, C.; Hansen, K.; Diederich, F.; Whetten, R. L. *Nature*, in press.
- (17) Olah, G. A., Ed. *Cage Hydrocarbons*; Wiley: New York, 1990.
- (18) For mass spectrometric detection of C_{60}^+ ions generated by kilo- and megaelectronvolt bombardment of polymers, see: (a) Feld, H.; Zurmühlen, R.; Leute, A.; Benninghoven, A. *J. Phys. Chem.* **1990**, *94*, 4595. (b) Brinkmann, G.; Barofsky, D.; Demirev, P.; Fenyö, D.; Håkansson, P.; Johnson, R. E.; Reimann, C. T.; Sundqvist, B. U. R. *Chem. Phys. Lett.* **1992**, *191*, 345.

Endohedral Rare-Earth Fullerene Complexes

Edward G. Gillan, Chahan Yeretizian, Kyu S. Min, Marcos M. Alvarez, Robert L. Whetten,* and Richard B. Kaner*

Department of Chemistry and Biochemistry and Solid State Science Center, University of California, Los Angeles, California 90024-1569 (Received: May 28, 1992; In Final Form: June 26, 1992)

The technique of carbon-arc evaporation has been successfully utilized to encapsulate a wide variety of rare-earth species in carbon cages. We have observed $M_m@C_n$ ($M = Ce, Nd, Sm, Eu, Gd, Tb, Dy, Ho, or Er$) species present in the toluene extracts of the carbon soot using laser desorption mass spectrometry. The presence of multiple-metal species appears to depend strongly on the metal-to-carbon atom ratio found in the starting rods, with the higher metal concentrations favoring multiple-metal incorporation. One often observed dimetallofullerene is $M_2@C_{80}$. Molecular orbital arguments are presented to support a possible icosahedral structure for C_{80} .

Introduction

The new family of hollow carbon cage molecules known as fullerenes has intrigued researchers since their discovery in 1985.¹ The insertion of atoms or ions inside the cages (endohedral incorporation) was first examined using laser vaporization techniques.^{2–5} Early photofragmentation studies provided strong evidence that the metals were inside the carbon cages.⁶ After a simple method for generating macroscopic quantities of fullerenes using a carbon evaporator was developed by Krätschmer, Huffman, et al. (K–H method),⁷ this technique was applied to the formation of endohedral metallofullerenes.^{8–13} These species appear to be soluble in common organic solvents including benzene, toluene, and carbon disulfide. Recent reports include the single-metal-containing fullerenes $La@C_{82}$,⁸ $Y@C_{82}$,^{5,9} $Sc@C_{82}$,¹² and $Fe@C_{60}$ ¹³ and the multiple-metal-containing fullerenes $La_2@C_{80}$,^{10,11} $Y_2@C_{82}$,^{5,9} and $Sc_3@C_{82}$.¹² EPR studies on $M@C_{82}$ species ($M = Sc, Y, or La$) demonstrate that the metals are in +3 oxidation states.^{9,12,15} Collision probes of $La_2@C_{80}$ and $Tb@C_{82}$ which yield no metal or fullerene fragments after impact with a silicon surface provide further evidence that the metals are strongly bound to the carbon cages.¹⁴

The fact that lanthanum can be successfully incorporated in fullerene cages suggests that other 4f block metals might be incorporated as well, owing to their similar electron configurations, oxidation states, ionic radii, and ionization potentials (see Table I). Here we report the successful encapsulation of cerium (Ce), neodymium (Nd), samarium (Sm), europium (Eu), gadolinium (Gd), terbium (Tb), dysprosium (Dy), holmium (Ho), and erbium (Er) in fullerene cages using carbon-arc evaporation techniques. Our studies indicate that if the metals or their ions formed from metal oxide evaporation are present in sufficient quantities during fullerene formation, some become trapped inside the carbon cages.

Higher concentrations of metal oxide lead to some multiple-metal encapsulation.

Experimental Methods

The gravity-driven resistive heating apparatus used has been described previously.¹⁰ In each case, metal oxides were mixed with graphite cement (HTGC-Dylon Industries) forming a thick paste which was pressed into 1.5 in. by 0.125 in. graphite rods (Poco Graphite Inc.) that had been hollowed out to 1.25 in. using a 0.056-in. drill bit. The metal oxide loadings were optimized to balance a high metal oxide content with a paste viscous enough to be pressed into the rods. The metal oxides and the metal-to-carbon atomic ratios for the rods were as follows: CeO_2 (99.9% Alpha), 1.0 Ce/100 C; Nd_2O_3 (99.9% Alpha) 1.1 Nd/100 C; Sm_2O_3 (Matheson Co.), 0.9 Sm/100 C; Eu_2O_3 (99.99% Alpha), 0.8 Eu/100 C; Gd_2O_3 (99.9% Atomergic), 1.0 Gd/100 C; Tb_4O_7 (99.9% Research Chemicals), 1.4 Tb/100 C; Dy_2O_3 (99.9% Atomergic), 1.5 Dy/100 C; Ho_2O_3 (99.9% Atomergic), 1.9 Ho/100 C; Er_2O_3 (96% Pechiney), 2.0 Er/100 C. All starting oxides were phase pure as indicated by powder X-ray diffraction. The metal oxide containing rods were cured at 200 °C for 1 day followed by heating at 900 °C under vacuum for at least 1 day. The soot produced by the resistive heating of these rods was refluxed in boiling toluene to extract fullerene and metallofullerene species. All samples were handled in air without special precaution. The toluene extracts were analyzed by a laser-desorption mass spectrometry (LDMS) procedure described previously.¹⁹ Radiation pulses (10^{-8} s) from an ArF laser operating at 193 nm (6.4 eV) were used to desorb the species from coated stainless steel rods and the positive ions formed were detected by a reflection mass spectrometer. Additionally for Eu, Gd, and Tb a Nd:YAG laser operating at 266 nm (4.7 eV) was used to obtain spectra.